The dissipative dynamics of a pair of paraelectric tunnelling impurities

1996 J. Phys.: Condens. Matter 8 7303

(http://iopscience.iop.org/0953-8984/8/39/007)

J. Phys.: Condens. Matter **8** (1996) 7303–7320. Printed in the UK

The dissipative dynamics of a pair of paraelectric tunnelling impurities

Orestis Terzidis† and Alois Würger‡

† Institut für Theoretische Physik, Universität Heidelberg, Philosophenweg 19, 69120 Heidelberg, Germany

‡ Institut Laue–Langevin Avenue des Martyrs, BP 156, 38042 Grenoble Cédex 09, France

Received 1 February 1996, in final form 17 May 1996

Abstract. Paraelectric impurities contribute significantly to the low-temperature properties of alkali halide crystals. Even at very low density the dipolar interaction of adjacent defect ions may lead to deviations from the behaviour expected for isolated impurities; in a certain range of concentration it is sufficient to consider pairs of coupled defects. Applying a projection operator method, previous work on this pair model is extended to the case of finite asymmetry and weak coupling to acoustic phonons. After performing the ensemble averaging, the specific heat and the zero-frequency susceptibility are calculated and compared with experimental data on KCl:Li and KCl:CN. The isotope effect on the Rabi frequency and relaxation rate is discussed.

1. Introduction

Quantum tunnelling of substitutional defect ions in alkali halide crystals leads to particular low-temperature properties [1, 2]. As a standard example one may think of potassium chloride doped with a small amount of lithium (KCl:Li). Because of its smaller radius, the lithium ion experiences a potential energy landscape quite different from that of the potassium. As a consequence it does not stay on the lattice site but prefers one of eight equivalent off-centre positions on the corners of a cube of side length $d = 1.4$ Å and with the original potassium site at its centre [3]. Tunnelling between these states gives rise to a characteristic ground-state splitting.

There are three different matrix elements for tunnelling along the edges of the cube, along a face diagonal, and along a space diagonal. The first one dominates the tunnelling spectrum, since in this case the distance between equilibrium states is smallest and the potential barrier is lowest [3]. This fact leads to a significant simplification: when neglecting face and space diagonal tunnelling, the partition function of the eight-level system is given by the third power of the partition function of a two-level system, and the linear response to a time-dependent electric field is identical to that of a two-level system. Hence one is led to mimic the tunnelling defect by a spin-$\frac{1}{2}$ system, which is of course much simpler to deal with than the original eight-dimensional problem [4, 5].

Nearby defect ions interact strongly, through both electric dipole and elastic strain fields [6, 7, 8]. Even at concentrations as low as 60 ppm, most physical properties show significant interaction effects; as examples we note the broadening of the Schottky peak in the specific heat [9] and low-energy excitations well below the tunnelling splitting [10]. For the case of zero bias, Kranjc considered coupling to acoustic phonons in a small-polaron approach, and derived both a finite-phase coherence time and a reduced tunnel energy [12].

0953-8984/96/397303+18$19.50

Both the elastic and the electric interaction of adjacent impurities vary with the inverse cube of the distance of two defects; thus the average coupling increases with rising concentration. Two regimes are to be distinguished [13, 14].

(i) In the dilute case the average interaction energy is smaller than the tunnelling energy. Then most defects can be considered as isolated; only a few are sufficiently close to form strongly coupled pairs. Since the coupling energy may exceed the tunnelling energy by several orders of magnitude, it cannot be treated by perturbation theory with respect to the latter.

(ii) With rising concentration clusters of three and more defects occur with increasing probability. At some point the average interaction energy exceeds the tunnel splitting; accordingly the coupling to more than one neighbour becomes important, and the pair model breaks down [13].

In this paper we investigate pairs of interacting two-level tunnelling defects, corresponding to the dilute case (i). Previously we have derived the exact solution for the case where each defect moves in a symmetric potential [15]; in the present work we include both a finite asymmetry energy and coupling to phonons. The generalization to asymmetric potentials is essential for the description of recent experiments on tunnelling of coupled pairs of lithium ions in KCl [10]. The finite bias gives rise to a relaxation feature in the dynamical response function; thus damping arising from phonon coupling has to be taken into account.

The paper is organized as follows. In section 2 the model is specified. In section 3 some basic formulas of a projection formalism for the symmetrized correlation functions are stated. In section 4 the dynamics of a symmetric defect pair is derived within this framework and in section 5 damping rates due to phonon coupling are evaluated. Section 6 gives some information about the ensemble average. Section 7 considers the influence of a small asymmetry for strongly coupled pairs and in section 8 we discuss our results in view of various static and dynamical experiments for lithium and cyanide impurities.

2. The model

The Hamiltonian of the model considered in this paper consists of three parts,

$$H = H_S + H_B + H_{SB}. \tag{1}$$

The first one accounts for the 'system' consisting of a pair of two-state impurities:

$$H_S = \frac{\Delta_0}{2}\sigma_x + \frac{\Delta}{2}\sigma_z + \frac{\Delta_0'}{2}\tau_x + \frac{\Delta'}{2}\tau_z - \frac{1}{2}J\sigma_z\tau_z \tag{2}$$

with Pauli matrices σ_α and τ_α. The z-components correspond to the real-space coordinates. The two localized states of the first impurity are labelled by $\sigma_z = \pm 1$; they are separated in energy by the bias Δ. The off-diagonal part involves the quantum motion with the overlap tunnel matrix element Δ_0. The second impurity is described by the matrices τ_α and the energies Δ' and Δ_0'. The last term in equation (2) accounts for the dipolar interaction of the defects.

The remaining parts of the Hamiltonian involve the heat bath which consists of Debye phonons:

$$H_B = \sum_k \hbar\omega_k b_k^\dagger b_k \tag{3}$$

and which are linearly coupled to the impurity coordinates:

$$H_{SB} = \frac{1}{2}(\sigma_z + \tau_z)e \tag{4}$$

with the elastic distortion

$$e = \sum_k \hbar\lambda_k (b_k^\dagger + b_k). \tag{5}$$

The coupling constants λ_k depend linearly on the square root of the wave vector k; for acoustic phonons one finds with $\omega_k = ck$ the well known expression

$$\lambda_k = \frac{\gamma}{\hbar}\sqrt{\frac{\hbar\omega_k}{2mc^2}}. \tag{6}$$

The coupled density of states of Debye phonons yields a spectral function

$$J(\omega) = \sum_k \lambda_k^2 \delta(\omega - \omega_k) = \frac{\gamma^2}{\hbar m c^2 \omega_D^3}\ \omega^3\ \Theta(\omega_D - \omega) \tag{7}$$

with a characteristic cubic frequency dependence; we have introduced the oscillator frequencies ω_k, Debye frequency ω_D, elastic coupling energy γ, and sound velocity c. The phonon coupling of substitutional defects, like Li in K:Cl, is in general well described by the cubic spectral density (7). (For a discussion of the selection rules for the eight-state system see reference [17]. A different situation may be encountered for interstitial defects, where the above coupling term may be absent due to the local site symmetry, thus requiring a more careful investigation [18].)

According to the two-state approximation for each impurity, the system operator H_S is formulated in terms of Pauli matrices σ_α, τ_α. Since all lattice sites are identical, different tunnelling amplitudes can arise only from different impurities. For the two stable lithium isotopes in KCl one finds $\Delta_0 \approx 1.1$ K for ^{7}Li and $\Delta_0 \approx 1.65$ K for ^{6}Li. The resulting isotope effect has been studied in detail in reference [30]. In this paper we will confine ourselves to pairs of the same mass; hence we put $\Delta_0 = \Delta_0'$. The case of different defects leads to more complicated formulas without changing the essential physics [16].

The dipolar interaction varies with the inverse cube of the defect distance:

$$\frac{1}{2}J = \pm\frac{1}{4\pi\epsilon_0\epsilon_r}\ \frac{q^2d^2}{r^3} \tag{8}$$

where $p = \frac{1}{2}qd$ denotes the absolute value of the dipole moment connected to the pseudo-spins, $\boldsymbol{p} = \frac{1}{2}qd\sigma_z$. The two signs mimic the dependence of the dipolar energy on the relative orientation of the dipole moments. The interaction term $-\frac{1}{2}J\sigma_z\tau_z$ leads to either a parallel orientation ($J > 0$) or an antiparallel orientation ($J < 0$) of the dipole moments. This sign effect will play a significant role whenever the pair interacts with acoustic or microwaves with a wavelength much larger than the distance of the two defects; parallel orientation leads to constructive, antiparallel to a destructive interference [15].

Assuming a random distribution of the defects on the host lattice, Klein obtained for the distribution function of the coupling energy [5]

$$P(J) = \text{constant} \times J^{-2} \qquad \text{for } J_1 \leqslant |J| \leqslant J_2 \tag{9}$$

with most systems being close to the lower bound. In the following we refer to $|J| \ll \Delta_0$ and $\Delta_0 \ll |J|$ as the cases of weak and strong coupling, respectively. We postpone a detailed discussion of the distribution to section 7. Here let us only state that the upper bound J_2 is of the order of 100 K; with the impurity concentration c one has for the lower

bound $J_1 = cJ_2$. Thus for defect concentrations below 100 ppm, most pairs are weakly coupled, and only a small fraction of them show strong coupling. Clearly in our approach we do not account for strongly coupled triples and larger clusters. Yet such configurations are very rare at sufficiently low density. The pair model breaks down as soon as the average interaction energy J_1 is comparable to the tunnel energy Δ_0 [17].

Whereas the coupling energy J accounts for the nearest-neighbour impurity, the interaction with additional defects and with lattice imperfections is subsumed in the asymmetry energy Δ. Specific heat and susceptibility data for KCl:Li show the average bias to be much smaller than the tunnel energy, $\Delta \ll \Delta_0$. Hence the bias is irrelevant for weakly coupled defects whose level splittings are of the order of Δ_0. Yet pairs of nearby impurities exhibit low-energy excitations of the order of Δ_0^2/J which may be significantly affected by a small but finite bias. In such a case, however, the source of the bias is far away as compared to the impurity distance; as a consequence, the corresponding dielectric or elastic strain fields are the same at the two impurity sites, resulting in equal asymmetry energies. (For the case of two eight-state impurities, this has been discussed in detail in references [30, 17].) Accordingly we put $\Delta = \Delta'$ throughout this paper.

3. Projection formalism

The essential idea of the projection formalism (proposed by Mori [25] and Zwanzig [26]) is to consider the linear space spanned by the operators σ_α, τ_α, b_k, $b_k^\dagger$ and their products, with the scalar product $(A|B)$. Several different definitions for the inner product are possible; in this article we use

$$(A|B) = \frac{1}{2}\langle A^\dagger B + BA^\dagger\rangle \tag{10}$$

where the angular brackets indicate the canonical average $\langle\cdots\rangle = \mathrm{tr}\{\cdots W\}$ with $W = \mathrm{e}^{-\beta H}/\mathrm{tr}\{\mathrm{e}^{-\beta H}\}$. In the following we consider symmetrized two-time correlation functions

$$C_{\mu\nu}(t) = (A_\mu(t)|A_\nu). \tag{11}$$

Time evolution of any operator A_μ is governed by the Heisenberg equation

$$\bar{h}\partial_t A_\mu = \mathrm{i}[H, A_\mu] = \mathrm{i}\bar{h}\mathcal{L}A_\mu \tag{12}$$

which defines the Liouvillian $\mathcal{L}$ acting on the linear space of quantum mechanical operators. The formal integral of (12), $\exp(\mathrm{i}\mathcal{L}t)$, in general involves the whole space $\{A_\nu\}$ where ν labels a complete set.

Following Mori and Zwanzig, we split this space into the subspace of system operators and its complement, the latter including both pure bath and composite system–bath operators. In order to make this idea more precise we introduce a projection operator P on the subspace spanned by the set of system operators $\{p_\mu\}$:

$$P = \sum_{\mu,\nu} |p_\mu)\eta_{\mu\nu}(p_\nu| \qquad Q = 1 - P. \tag{13}$$

The operator Q projects on the complement. The metric tensor η is defined as the inverse correlation matrix at time zero

$$M_{\mu\nu} = (p_\mu|p_\nu) = (\eta^{-1})_{\mu\nu}. \tag{14}$$

(In the following we will use the term 'metric tensor' for both η and M.) At this point the choice of the symmetric scalar product (10) becomes clear; for Pauli matrices we have $\langle\sigma_\mu\sigma_\nu + \sigma_\nu\sigma_\mu\rangle = 2\delta_{\mu\nu}$.

Making use of the projectors (13) one can split up the Heisenberg equations into two parts:

$$P\dot{A}_\mu = \mathrm{i}\, P\mathcal{L}P\, A_\mu + \mathrm{i}\, P\mathcal{L}Q\, A_\mu \tag{15}$$

$$Q\dot{A}_\mu = \mathrm{i}\, Q\mathcal{L}P\, A_\mu + \mathrm{i}\, Q\mathcal{L}Q\, A_\mu. \tag{16}$$

After integrating the second of these equations and making use of (11) one ends up with an effective equation of motion for symmetrized correlation functions:

$$\partial_t\, C_{\mu\nu}(t) = -\mathrm{i}\,\Omega_{\mu\kappa} C_{\kappa\nu}(t) - \int_0^t \mathrm{d}t'\, K_{\mu\kappa}(t-t') C_{\kappa\nu}(t'). \tag{17}$$

Using the Laplace transformation

$$C_{\mu\nu}(z) = \mathrm{i}\int_0^\infty \mathrm{d}t\; C_{\mu\nu}(t)\,\mathrm{e}^{\mathrm{i}zt} \qquad \mathrm{Im}(z) > 0 \tag{18}$$

the correlation functions are given by the matrix equation

$$C(z) = \frac{-1}{z - \Omega + K(z)}\, M. \tag{19}$$

Here the frequency matrix is determined by the energy differences of the system

$$\Omega_{\mu\kappa} = (s_\mu | P\mathcal{L}P\, s_\lambda)\, \eta_{\lambda\kappa} \tag{20}$$

and the memory functions

$$K_{\mu\kappa}(z) = (s_\mu | P\mathcal{L}Q\, \frac{1}{Q\mathcal{L}Q - z}\, Q\mathcal{L}P | s_\nu)\, \eta_{\nu\kappa} \tag{21}$$

reflect the influence of the bath. The above resolvent formula may be modified by an arbitrary unitary transformation U to

$$C(z) = U\, \frac{-1}{z - U^\dagger \Omega U + U^\dagger K(z) U} U^\dagger M U\, U^\dagger. \tag{22}$$

The interesting point about this formula is that the two essential items of information may be separated: the resonance frequencies and damping rates are given by the zeros of the denominator and the corresponding residues by the numerator.

Since the matrices Ω and M commute, there is a particular unitary transformation which diagonalizes both; for the case of zero asymmetry it is given explicitly in appendix A. This solution provides a useful starting point for an approximative treatment of the full problem with finite bias and phonon coupling; it will permit us to write both resonances and residues of equation (22) as power series in terms of a well defined small parameter.

The Liouville space of the pair model introduced in section 2 is spanned by all possible products of the two spins and the identity:

$$\begin{array}{llll}
(1)\ p_1 = \sigma_y & p_2 = \sigma_z & p_3 = \sigma_x\tau_y & p_4 = \sigma_x\tau_z \\
(2)\ p_5 = \tau_y & p_6 = \tau_z & p_7 = \sigma_y\tau_x & p_8 = \sigma_z\tau_x \\
(3)\ p_9 = \sigma_y\tau_z & p_{10} = \sigma_z\tau_y & p_{11} = \sigma_x & p_{12} = \tau_x \\
(4)\ p_{13} = \sigma_z\tau_z & p_{14} = \sigma_y\tau_y & p_{15} = \sigma_x\tau_x & p_{16} = 1.
\end{array} \tag{23}$$

All operators acting on elements of the Liouville space are represented by 16×16 matrices with respect to this basis. For later convenience we have split that set into the four groups.

4. The symmetric defect pair

In this section we consider the symmetric problem without phonon coupling, i.e. we put $\Delta = 0 = \Delta'$ and $H_{SB} = 0$ and thus have

$$H = \frac{\Delta_0}{2}\sigma_x + \frac{\Delta_0}{2}\tau_x - \frac{1}{2}J\sigma_z\tau_z. \tag{24}$$

Products of localized states for each spin provide a physical basis of quantum states. Putting e.g. $|lr\rangle$ for the state with the σ-spin in its left-hand well and the τ-spin in its right-hand well, there are four localized states $|ll\rangle$, $|rr\rangle$, $|lr\rangle$, and $|rl\rangle$.

The spectrum of (24) comprises the four levels $\pm\frac{1}{2}J$ and $\pm(\frac{1}{4}J^2 + \Delta_0^2)^{1/2}$. Using the abbreviations

$$\eta_\pm = \pm J/2 + \sqrt{J^2/4 + \Delta_0^2} \qquad w_\pm = \sqrt{\frac{\eta_\pm}{\eta_+ + \eta_-}} \tag{25}$$

we find for the energies and the corresponding eigenstates

$$\begin{aligned}
E_3 &= \frac{1}{2}(\eta_+ + \eta_-)\colon\ |3\rangle = 2^{-1/2}\left[w_+\{|lr\rangle + |rl\rangle\} + w_-\{|ll\rangle + |rr\rangle\}\right] \\
E_2 &= \frac{1}{2}(\eta_+ - \eta_-)\colon\ |2\rangle = 2^{-1/2}\{|lr\rangle - |rl\rangle\} \\
E_1 &= -\frac{1}{2}(\eta_+ - \eta_-)\colon\ |1\rangle = 2^{-1/2}\{|ll\rangle - |rr\rangle\} \\
E_0 &= -\frac{1}{2}(\eta_+ + \eta_-)\colon\ |0\rangle = 2^{-1/2}\left[w_-\{|lr\rangle + |rl\rangle\} - w_+\{|ll\rangle + |rr\rangle\}\right].
\end{aligned} \tag{26}$$

The energy differences $\eta_\pm$ are most relevant for spectroscopy; for large J they are well approximated by the first term of the power series

$$\eta_+ = J[1 + \mathrm{O}(\Delta_0^2/J^2)] \qquad \eta_- = \frac{\Delta_0^2}{J}[1 + \mathrm{O}(\Delta_0^2/J^2)]. \tag{27}$$

The root w_+ tends to one whereas w_- vanishes in the strong-coupling limit $\Delta_0/J \to 0$. (Here and in the following we assume J positive if not stated otherwise.)

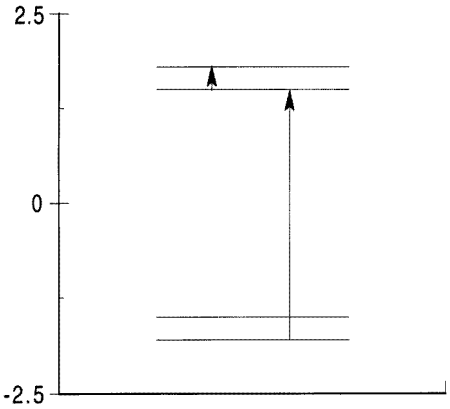

Figure 1. The energy spectrum of a pair of two-level systems The arrows indicate the allowed dipole transitions for $J > \Delta_0$.

The two low-lying eigenstates obviously correspond to essentially parallel configurations $|ll\rangle \pm |rr\rangle$; the antiparallel admixture with amplitude w_- becomes negligible for strong interactions. In the same sense the two upper levels correspond to antiparallel configurations $|lr\rangle \pm |rl\rangle$. It is worth noting that a negative interaction would lead to an inverse situation, i.e. low-lying antiparallel and higher parallel states (antiferromagnetic coupling). It is also worth noting that the four levels somehow appear in two level pairs as visualized in figure 1: it costs little energy just to change the symmetry of the wave function but much energy to change from parallel to antiparallel constellations.

The fact that one can write down explicitly the eigenstates of the energy operator makes it clear that there is an exact solution to the problem [15]. In this paper we choose the projection formalism in order to develop this solution because this gives a basis for the calculation of the memory function.

Discarding the phonon coupling, the correlation matrix is determined by frequency and metric matrices. The former reads

$$\Omega = \begin{pmatrix} \hat{\Omega}_{11} & 0 & 0 & 0 \\ 0 & \hat{\Omega}_{22} & 0 & 0 \\ 0 & 0 & \hat{\Omega}_{33} & \hat{\Omega}_{34} \\ 0 & 0 & \hat{\Omega}_{34}^{\dagger} & \hat{\Omega}_{44} \end{pmatrix} \tag{28}$$

whose entries $\hat{\Omega}_{ij}$ are 4×4 matrices with labels referring to the four groups in equation (23).

Calculating the metric tensor M according to (14) requires the statistical operator which has been derived previously [15]; in the present notation it reads

$$W = \frac{1}{4}\Big[1 + t_+ t_- \sigma_x \tau_x - w_- w_+ (t_+ + t_-)(\sigma_x + \tau_x) + (w_-^2 t_+ - w_+^2 t_-)\sigma_y \tau_y + (w_+^2 t_+ - w_-^2 t_-)\sigma_z \tau_z\Big] \tag{29}$$

with the temperature factors

$$t_\pm = \tanh\left(\frac{\beta \eta_\pm}{2}\right). \tag{30}$$

The expectation value of any operator is given by $\langle p_j \rangle = \mathrm{tr}(W p_j)$. With (14) and (23) we find

$$M = \begin{pmatrix} \hat{M}_{11} & \hat{M}_{12} & 0 & 0 \\ \hat{M}_{12}^{\dagger} & \hat{M}_{22} & 0 & 0 \\ 0 & 0 & \hat{M}_{33} & \hat{M}_{34} \\ 0 & 0 & \hat{M}_{34}^{\dagger} & \hat{M}_{44} \end{pmatrix} \tag{31}$$

with 4×4 matrices $\hat{M}_{ij}$ that are easily calculated. Both the metric tensor and the frequency matrix split into two 8×8 blocks which simplifies the problem substantially. This simplification is removed by a finite asymmetry energy.

For the choice of the scalar product (10) the frequency matrix always commutes with the metric tensor; hence there is a unitary transformation U acting on the Liouville space that diagonalizes both. Indeed this transformation can be calculated explicitly for the symmetric pair and is given in appendix A.

The eigenvalues of Ω and M, i.e. the frequencies and their corresponding metric factors

are given by the following list:

$$\begin{array}{ll}
\pm\eta_- & 1+t_+ \\
\pm\eta_- & 1-t_+ \\
\pm\eta_+ & 1+t_- \\
\pm\eta_+ & 1-t_- \\
\pm(\eta_+ + \eta_-) & 1+t_+t_- \\
\pm(\eta_+ - \eta_-) & 1-t_+t_- \\
0 & (1+t_+)(1+t_-) \\
0 & (1-t_+)(1-t_-) \\
0 & (1+t_+)(1-t_-) \\
0 & (1-t_+)(1+t_-).
\end{array} \tag{32}$$

(Note that the metric discriminates between degenerate frequencies.)

Having found the appropriate unitary transformation, any entry of the 16×16-dimensional correlation matrix can be calculated by use of formula (22). (Formally this corresponds to an expansion of the elements of (23) in terms of the eigenvectors of Ω and M.) As examples we quote the σ_z–σ_z-correlation

$$C_{2,2}(z) = -w_-^2 \frac{z}{z^2 - \eta_+^2/\hbar^2} - w_+^2 \frac{z}{z^2 - \eta_-^2/\hbar^2} \tag{33}$$

and the σ_z–τ_z-correlation

$$C_{2,6}(z) = t_- w_-^2 \frac{z}{z^2 - \eta_+^2/\hbar^2} - t_+ w_+^2 \frac{z}{z^2 - \eta_-^2/\hbar^2} \tag{34}$$

and also the σ_x–σ_x-correlation

$$\begin{aligned} C_{11,11}(z) = {} & -2\, w_-^2\, w_+^2 (1 + t_+t_-)\frac{1}{z} - \frac{1}{2}(w_-^2 - w_+^2)^2(1 + t_+t_-)\, \frac{z}{z^2 - (\eta_- + \eta_+)^2/\hbar^2} \\ & - \frac{1}{2}(1 - t_+t_-)\frac{z}{z^2 - (\eta_- - \eta_+)^2/\hbar^2}. \end{aligned} \tag{35}$$

With $\boldsymbol{P} = \frac{1}{2} q \boldsymbol{d}(\sigma_z + \tau_z)$ the spectrum of the dielectric response function

$$\alpha(t - t') = (\mathrm{i}/\epsilon_0)\langle[\boldsymbol{P}(t), \boldsymbol{P}(t')]\rangle \Theta(t - t') \tag{36}$$

is connected via the fluctuation-dissipation theorem

$$\alpha''(\omega) = (2/\epsilon_0)(qd/2)^2 \tanh(\beta\hbar\omega/2)(C''_{22}(\omega) + C''_{66}(\omega) + C''_{26}(\omega) + C''_{62}(\omega)) \tag{37}$$

to the correlation spectra $C''_{ij}(\omega) = \mathrm{Im}\, C_{ij}(\omega + \mathrm{i}\eta)$. With equations (33) and (34) one is led to the response function

$$\alpha(t) = (2\epsilon_0)(qd/2)^2 \sum_{\pm} w_{\mp}^2 [1 + \mathrm{sgn}(J) t_{\mp}] t_{\pm} \sin(\eta_{\pm} t/\hbar)\Theta(t). \tag{38}$$

This result has been discussed previously in reference [15].

5. Damping rates

Now we turn to the interaction with the phonon bath. Assuming weak coupling we evaluate the memory matrix (21) in lowest-order perturbation theory; we retain only its dissipative part and hence discard the renormalization of the tunnel energy. (For a discussion on this point see, e.g., references [12, 17].)

In the lowest Born approximation the memory matrix reads in the time representation

$$K_{\mu\kappa}(t-t') = (p_\mu|P\mathcal{L}_{SB}Q\mathrm{e}^{-\mathrm{i}\mathcal{L}_0(t-t')}Q\mathcal{L}_{SB}P|p_\nu)_0\,\eta^0_{\nu\kappa}. \tag{39}$$

This formula states: at time t' the system is scattered by the interaction $P\mathcal{L}_{SB}Q$ into the complement space Q, then propagates according to the uncoupled time evolution operator, and is scattered back to the system space P at time t.

The damping rates are found by linearizing the eigenvalue equation $|z-\Omega+\mathrm{i}K''(z)|$ in terms of $K''(z)$ and by evaluating the memory function at the bare poles.

In order to proceed further we expand $Q\mathcal{L}_{SB}p_\mu$ in terms of the elements (23) times the elastic strain e. Both the thermal average $(.|.)_0$ and the metric tensor η^0 are calculated with the uncoupled Hamiltonian H_0; thus equation (39) factorizes into a spin part and a bath part. Putting

$$\epsilon_{\mu\mu'} = \frac{1}{4}\,\mathrm{tr}\{[\sigma_z+\tau_z,\,p_\mu]p_{\mu'}\} \tag{40}$$

permits us to rewrite the matrix elements $K_{\mu\nu}$ as

$$K_{\mu\kappa}(t-t') = \frac{1}{2}\sum_{\mu',\nu'}\epsilon_{\mu\mu'}\epsilon_{\nu\nu'}(\langle p_{\mu'}(t)\,p_{\nu'}(t')\rangle_0\langle e(t)e(t')\rangle_0 + \langle p_{\nu'}(t')\,p_{\mu'}(t)\rangle_0\langle e(t')e(t)\rangle_0)\eta_{\nu'\kappa}. \tag{41}$$

Inserting the relation for the spectra of ordinary and symmetrized correlation functions

$$\frac{1}{2}\int_{-\infty}^{\infty}\mathrm{d}t\;\mathrm{e}^{\mathrm{i}\omega t}\langle A(\pm t)A\rangle = \frac{2}{1+\mathrm{e}^{\mp\beta\hbar\omega}}C''_A(\omega) \tag{42}$$

(with $C_A(t) = (A(t)|A)$) and the bath spectral function

$$B''(\omega) = \frac{1}{2}\int\mathrm{d}t\;\mathrm{e}^{\mathrm{i}\omega t}(e(t)|e) = \frac{\pi}{2}\,J(\omega)\coth(\beta\hbar\omega/2) \tag{43}$$

in the Fourier transform of equation (41), we find the memory function

$$K''_{\mu\kappa}(\omega) = \sum_{\mu',\nu'}\epsilon_{\mu\mu'}\epsilon_{\nu\nu'}\Sigma_{\mu'\nu'}(\omega)\eta_{\nu'\kappa} \tag{44}$$

to be determined by the weighted convolution integral

$$\Sigma''_{\mu\nu}(\omega) = \frac{2}{\pi}\int\mathrm{d}\Omega\;f(\omega,\Omega)C^{0\prime\prime}_{\mu\nu}(\omega-\Omega)\,B''(\Omega) \tag{45}$$

with the thermal factor

$$f(\omega,\Omega) = \frac{\cosh(\beta\hbar\omega/2)}{2\cosh(\beta\hbar\Omega/2)\cosh(\beta\hbar(\omega-\Omega)/2)} \tag{46}$$

arising from relation (42).

Like the frequency and metric matrices, the memory matrix splits in two 8×8 blocks. Since the damping rates are expected to be much smaller than the energies $\eta_\pm$, we linearize the zeros of the determinant $|z-\Omega+\mathrm{i}K''(z)|$ in terms of K; this amounts to keeping only the diagonal elements of the transformed matrix

$$U_I K_I U_I^\dagger U_I \eta_I U_I^\dagger. \tag{47}$$

Thus the poles in equation (32) acquire an imaginary part; the degeneracy of the frequencies $\eta_\pm/\hbar$ is lifted. The relevant correlation functions (33) and (34) involve the first four entries in equation (32); hence we restrict the explicit evaluation to corresponding damping rates. The rate of the first pole is given by

$$\begin{aligned}\gamma_1 = \int \mathrm{d}\Omega\, f(\omega,\Omega) J(\omega-\Omega) \coth\!\left(\frac{\beta\hbar(\omega-\Omega)}{2}\right) \frac{1}{1+t_+} \\ \times \Bigg[\frac{1}{2} w_-^2 (C^{0\prime\prime}_{9,10}(\Omega) + 2\mathrm{i}C^{0\prime\prime}_{9,11}(\Omega) + C^{0\prime\prime}_{11,12}(\Omega) \\ + \mathrm{i}C^{0\prime\prime}_{9,12}(\Omega) + \mathrm{i}C^{0\prime\prime}_{10,11}(\Omega) + C^{0\prime\prime}_{11,11}(\Omega) + C^{0\prime\prime}_{9,9}(\Omega)) \\ + \frac{3}{2} w_- w_+ (C^{0\prime\prime}_{11,14}(\Omega) - C^{0\prime\prime}_{11,15}(\Omega) + \mathrm{i}C^{0\prime\prime}_{9,14}(\Omega) - \mathrm{i}C^{0\prime\prime}_{9,15}(\Omega)) \\ + \frac{1}{2} w_- w_+ (C^{0\prime\prime}_{12,14}(\Omega) - C^{0\prime\prime}_{12,15}(\Omega) + \mathrm{i}C^{0\prime\prime}_{10,14}(\Omega) - \mathrm{i}C^{0\prime\prime}_{10,15}(\Omega)) \\ + w_-^2 (C^{0\prime\prime}_{14,14}(\Omega) + C^{0\prime\prime}_{15,15}(\omega-\Omega) - 2C^{0\prime\prime}_{14,15}(\Omega)) \Bigg]_{\hbar\omega=\eta_-}.\end{aligned} \tag{48}$$

After inserting the bare correlation functions, this rather complicated formula reduces to

$$\begin{aligned}\gamma_1 = \int \mathrm{d}\Omega\, f(\omega,\Omega) J(\Omega) \coth\!\left(\frac{\beta\hbar\Omega}{2}\right) \\ \times \left[\pi w_-^2 \frac{1+t_+t_-}{1+t_+} \delta(\omega-\Omega-\eta_+/\hbar-\eta_-/\hbar) + 2\pi w_+^2 \delta(\omega-\Omega) \right]_{\hbar\omega=\eta_-}\end{aligned} \tag{49}$$

and finally yields the imaginary part of the first η_--pole in (32):

$$\gamma_1 = \frac{\pi}{2} w_-^2 J(\eta_+/\hbar) \left\{ \coth\!\left(\frac{\beta\eta_+}{2}\right) - 1 \right\} + \pi w_+^2 J(\eta_-/\hbar) \coth\!\left(\frac{\beta\eta_-}{2}\right). \tag{50}$$

Similar expressions appear for the other rates; we refrain from repeating the above argument, but simply note the resulting rates. Hence we find for the second pole in (32)

$$\gamma_2 = \frac{\pi}{2} w_-^2 J(\eta_+) \left\{ \coth\!\left(\frac{\beta\eta_+}{2}\right) + 1 \right\}. \tag{51}$$

The rates for the large frequency $\eta_+/\hbar$, i.e. for the third and fourth pole pairs, are given by

$$\gamma_3 = \frac{\pi}{2} w_+ J(\eta_-/\hbar) \left\{ \coth\!\left(\frac{\beta\eta_-}{2}\right) + 1 \right\} + \pi w_- J(\eta_+/\hbar) \coth\!\left(\frac{\beta\eta_+}{2}\right) \tag{52}$$

and

$$\gamma_4 = \frac{\pi}{2} w_+ J(\eta_-/\hbar) \left\{ \coth\!\left(\frac{\beta\eta_-}{2}\right) - 1 \right\}. \tag{53}$$

From the factor $[1+\mathrm{sgn}(J)]t_\pm$ in (38) one finds that the response function involves either the first and the third, or the second and the fourth poles of (32), depending on the sign of J. For the most physical case $J > 0$, the first case is realized; accordingly γ_1 and γ_3 are the relevant damping rates for the two signs in (38).

As is easily inferred from the metric factors $(1 \pm t_+)$, the first two poles in (32) correspond to tunnelling within the ground-state doublet and within the upper doublet, respectively. At low temperature $k_\mathrm{B}T \ll \eta_+$ we find $1+t_+ \approx 2$ and $1-t_+ \approx \mathrm{e}^{-\beta\eta_+} \ll 1$; then the upper level is almost completely depopulated. The most relevant rate γ_1 then reads

$$\gamma_1 = \pi J(\eta_-/\hbar) \coth\!\left(\frac{\beta\eta_-}{2}\right). \tag{54}$$

Taking into account the selection rules shown in figure 1, the rates $\gamma_1, \ldots, \gamma_4$ could actually be derived quite simply by means of Fermi's golden rule; yet this approach fails when considering the most interesting case of a finite asymmetry energy. Moreover, the projection method yields both amplitudes and temperature factors in an unambiguous fashion.

6. Small asymmetry and strong coupling

In this section we want to discuss the effect of a finite asymmetry energy. For simplicity and since this seems to be the most relevant case [30, 17], we assume both defects to be subject to the same bias:

$$H = \frac{\Delta_0}{2}(\sigma_x + \tau_x) + \frac{\Delta}{2}(\sigma_z + \tau_z) - \frac{J}{2}\sigma_z\tau_z. \tag{55}$$

The asymmetry Δ is generally assumed to be much smaller than the tunnel energy. For uncoupled defects it is hence justified to consider the bias as a small perturbation. Yet the situation becomes different as soon as the interaction plays a significant role. Then the condition

$$\Delta \ll \Delta_0 \ll J \tag{56}$$

can be translated as

$$\eta_-, \Delta \ll \eta_+. \tag{57}$$

This means that the usual perturbation approach is of no use: the unperturbed system has then two energy scales; one of them is of the same order as the additional energy appearing. In order to get a more concrete impression of the situation one should bear in mind that for KCl:Li the tunnelling frequency Δ_0 is roughly 1 K, the asymmetry Δ somewhere in the range of 50 mK and the maximal coupling constant is about 100 K.

Thus one has to look for some approximation based on the relation (57). Consider the Hamiltonian (55) in the energy basis (26) of the symmetric pair:

$$\widetilde{H} = \begin{pmatrix} E_3 & 0 & w_-\Delta & 0 \\ 0 & E_2 & 0 & 0 \\ w_-\Delta & 0 & E_1 & w_+\Delta \\ 0 & 0 & w_+\Delta & E_0 \end{pmatrix} \tag{58}$$

which obviously is diagonal for zero bias, $\Delta = 0$. The spectrum (26) and relation (57) show that there are two pairs of nearby levels which are separated by the large energy $\eta_+ \approx J$.

According to (57) the lower 2×2 block involves off-diagonal entries $w_+\Delta$ which are comparable to the diagonal ones. From equation (25) we get $w_+ \approx 1$ and $w_- \approx \Delta_0^2/J^2 \ll 1$. Hence the remaining off-diagonal terms $w_-\Delta$ are smaller by a factor of Δ_0^2/J^2, and mix states from far apart levels; the level shift resulting from $w_-\Delta$ is of the order of $\Delta^2\Delta_0^2/J^3$ and thus truly negligible.

Accordingly truncating the Hamiltonian $\widetilde{H}$ to its lower doublet, defining new two-state operators $\psi_x = |1\rangle\langle 1| - |0\rangle\langle 0|$ and $\psi_z = |1\rangle\langle 0| + |0\rangle\langle 1|$, and discarding the constant energy E_0, we have the effective two-level system

$$h = \frac{1}{2}\frac{\Delta_0^2}{J}\psi_x + \Delta\psi_z. \tag{59}$$

In the case of different defect parameters, as introduced in (2), $\Delta_0^2/2J$ has to be replaced by $\Delta_0\Delta_0'/2J$ and Δ by $(\Delta + \Delta')/2$.

From the Hamiltonian (1) defined in section 2 one finds that taking phonon coupling into account amounts to replacing the asymmetry energy Δ with $\Delta + e$; thus we may apply the well known results for a dissipative two-state system with finite asymmetry energy [28].

When neglecting small corrections in terms of Δ_0'/J, we find $\psi_z = |ll\rangle\langle ll| - |rr\rangle\langle rr|$. Hence the states $\psi_z = \pm 1$ correspond to both impurities localized either in the right-hand or left-hand wells, $|ll\rangle$ or $|rr\rangle$; the tunnelling motion driven by the term proportional to ψ_x involves both impurities.

Accordingly the correlation spectrum of the spin fluctuations

$$\hat{G}(t - t') = \frac{1}{2}\langle \psi_z(t)\psi_z(t') + \psi_z(t')\psi_z(t)\rangle - \langle \psi_z\rangle^2 \tag{60}$$

of such a system is given by

$$\hat{G}(z) = -\frac{\eta_-^2}{E^2}\frac{z + \mathrm{i}\gamma_t}{(z + \mathrm{i}\gamma_t)^2 - E^2} - \frac{4\Delta^2}{E^2/\hbar^2}\operatorname{sech}^2(\beta E/2)\frac{1}{z + \mathrm{i}\gamma_l} \tag{61}$$

with $\eta_- = \Delta_0^2/J$,

$$E = \sqrt{\eta_-^2 + 4\Delta^2} \tag{62}$$

and the longitudinal and transverse damping rates

$$\gamma_l = 2\gamma_t = \frac{\pi\gamma^2}{\hbar^4 mc^2\omega_D^3}\eta_-^2 E\coth(\beta E/2). \tag{63}$$

With the effective tunnel frequency $\eta_-/\hbar$ for coherent tunnelling of two defects, equation (61) is identical to the well known expression for a two-level system in glasses [28]. As to the transverse rate γ_t, a similar result has been derived previously by Kranjc [12]. This work accounts for the reduction of the tunnelling energy through the polaron or screening effect, which our approach fails to reproduce. (We have neglected this effect when dropping the real part of the memory function.)

More rigorously, the above result for the damping rate can be reproduced by considering the full 16×16 memory matrix. For the longitudinal rate we thus find the expression

$$\gamma_l = \cosh^2\left(\frac{\beta E}{2}\right)\int \mathrm{d}\Omega\ f(\omega,\Omega)J(\Omega)\coth\left(\frac{\beta\Omega}{2}\right)\frac{2\eta_-^2}{E^2} \times \left[C_{3,3}^{0\prime\prime}(\omega - \Omega) + C_{3,7}^{0\prime\prime}(\omega - \Omega)\right]_{\omega=0}. \tag{64}$$

Inserting the bare correlation functions

$$C_{3,3}^{0\prime\prime}(\omega) = C_{3,7}^{0\prime\prime}(\omega) = \frac{\pi}{2}\{\delta(\omega - \eta_-/\hbar) + \delta(\omega + \eta_-/\hbar)\} \tag{65}$$

confirms the above result.

Finally we note again that for different one-particle tunnel energies Δ_0 and Δ_0', the quantity Δ_0^2/J should be replaced with $\Delta_0\Delta_0'/J$; different asymmetry energies Δ and Δ' would require replacing Δ with $\frac{1}{2}(\Delta + \Delta')$.

7. The average over pairs

In this section we discuss the ensemble average arising from a random distribution of the defects on the host lattice. In order to keep the average tractable we confine ourselves to the case of zero bias, $\Delta = 0$.

From low-frequency microwave spectroscopy it is known that the asymmetry energy is small for most tunnelling systems $\Delta \ll \Delta_0$ [14]; via rotary echoes, coupled pairs with a

bias of about 50 mK have been detected [10]. Such small values are of little significance when calculating the specific heat or the average resonant susceptibility, thus justifying our neglecting the asymmetry energy.

Considering N defects on N_0 sites, there are $N/2$ pairs, each of which occupies an average volume $V_1 = \frac{8}{3}\pi R^3$, with R some average distance to the next neighbour. R is connected to the defect density $n = N/V$ through

$$R = \left(\frac{3}{4\pi}\frac{1}{n}\right)^{1/3}. \tag{66}$$

The actual spacing of a defect pair, r, will vary between the lattice constant a and an upper bound which is roughly equal to R; there is no pair with $r > R$ since all defects are already involved in a pair at a distance equal to or smaller than R. Dropping an insignificant factor $(1 - a^3/R^3)^{-1}$ one obtains the distribution

$$P(J) = cJ_2\frac{1}{J^2} \qquad \text{for } J_1 = cJ_2 \leqslant |J| \leqslant J_2 \tag{67}$$

where we have introduced the defect concentration $c = N/N_0$ and furthermore maximal and minimal couplings

$$J_1 = \frac{1}{2\pi\epsilon_0\epsilon_r}\frac{p^2}{R^3} \qquad J_2 = \frac{1}{2\pi\epsilon_0\epsilon_r}\frac{p^2}{a^3}. \tag{68}$$

(We have assumed the distance r to obey a homogeneous distribution instead of the actual discrete spacings of lattice sites.)

With the value $p = 0.55e$ Å for the dipole moment of a lithium impurity in KCl (cf. [19]), one obtains an upper cut-off $J_2/k_B \sim 1000$ K, which is three orders of magnitude larger than the tunnel energy. Yet the actual maximum interaction of defects on nearest-neighbour sites is significantly smaller, $J_{\mathrm{NN}} \approx 150$ K. Clearly, at such small spacings the continuous distribution (67) is not valid; this flaw, however, is of little consequence, since the relevant quantities are rather determined by the lower bound J_1.

Noting the average interaction energy $np^2/\epsilon_0\epsilon_r$, it is clear that for $np^2/\epsilon_0\epsilon_r \ll \Delta_0$ only a few strongly coupled pairs exist, whereas most of the systems are interacting weakly.

After expressing the coupling in terms of the energies (25)

$$J = \pm\frac{\eta_\pm^2 - \Delta_0^2}{\eta_\pm} \qquad \left|\frac{\mathrm{d}J}{\mathrm{d}\eta_\pm}\right| = \frac{\eta_\pm^2 + \Delta_0^2}{\eta_\pm^2} \tag{69}$$

the distribution (67) leads to the density of states

$$\rho(\eta) = \frac{1}{2}NJ_1\frac{\eta^2 + \Delta_0^2}{(\eta^2 - \Delta_0^2)^2} \tag{70}$$

whose two branches are bounded according to equations (25) and (67) and which satisfies $\int \mathrm{d}\eta\ \rho(\eta) = N$.

Noting that $\eta_+\eta_- = \Delta_0^2$ and changing to the variable $x = \eta/\Delta_0$ permits us to express the average with respect to η of a quantity A as an integral:

$$\bar{A} = N\frac{cJ_2}{2\Delta_0}\int_{x_1}^{x_2}\mathrm{d}x\ \frac{1+x^2}{(1-x^2)^2}\{A(x) + A(1/x)\} \tag{71}$$

where the two terms in brackets arise from the two branches of the density of states $\rho(\eta)$. With the coupling constant

$$\mu = cJ_2/\Delta_0 \tag{72}$$

the bounds of the integral are given by

$$x_1 = -J_2/2\Delta_0 + \sqrt{(J_2/2\Delta_0)^2 + 1} \qquad x_2 = -\mu/2 + \sqrt{(\mu/2)^2 + 1}. \tag{73}$$

8. Discussion

Here we compare the results of the previous sections with various static and dynamic experiments on defect crystals in the low-density limit $\mu \ll 1$. According to section 7 the specific heat and low-frequency susceptibility may be discussed in terms of the zero-bias model, whereas for the Rabi frequency and the relaxation phenomenon a finite asymmetry energy has to be taken into account.

8.1. Specific heat

From the energy spectrum given by (25) one can easily calculate the partition function $Z = \cosh(\beta\eta_+/2)\cosh(\beta\eta_-/2)$ and the inner energy

$$U = -\frac{1}{2}\eta_- \tanh(\beta\eta_-/2) - \frac{1}{2}\eta_+ \tanh(\beta\eta_+/2) \tag{74}$$

of a coupled pair. The specific heat is obtained by taking the derivative of the latter with respect to temperature $T = 1/k_B\beta$ and to the average over all pair configurations:

$$c_V = 3\frac{1}{V}\sum_{\text{pairs}} \frac{\mathrm{d}U}{\mathrm{d}T}. \tag{75}$$

The factor 3 has been introduced in order to meet the correct expression for the actual eight-state system in the limit of vanishing coupling. Following section 7 we thus find

$$c_V = 3k_B N\mu \int_{x_1}^{x_2} \mathrm{d}x\ \frac{1+x^2}{(1-x^2)^2}\left\{\left(\frac{x\Delta_0}{2k_BT}\right)^2 \operatorname{sech}^2\left(\frac{x\Delta_0}{2k_BT}\right) + \left(\frac{\Delta_0}{2xk_BT}\right)^2 \operatorname{sech}^2\left(\frac{\Delta_0}{2xk_BT}\right)\right\}. \tag{76}$$

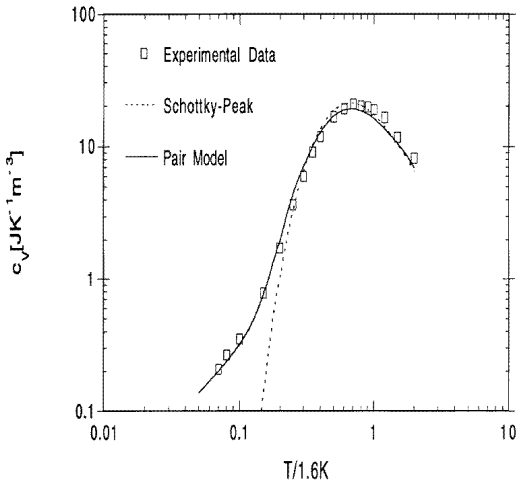

Figure 2. The specific heat for 73 ppm ^{6}Li in KCl. The data have been observed by Dobbs [27]. The full line gives the specific heat as obtained from the pair model, equation (76), and the dashed line that of isolated defects, equation (77).

In figure 2 we compare equation (76) with data observed for 73 ppm ^{6}Li in KCl [27] and with the specific heat of isolated defects,

$$c_{V_{\rm iso}} = 3k_{\rm B}\frac{N}{V}\left(\frac{\Delta_0}{2k_{\rm B}T}\right)^2 \operatorname{sech}^2\left(\frac{\Delta_0}{2k_{\rm B}T}\right). \tag{77}$$

Besides the narrowing of the Schottky peak there is a distinct excess specific heat at low temperature, which is well accounted for by the low-energy pair excitations in equation (76).

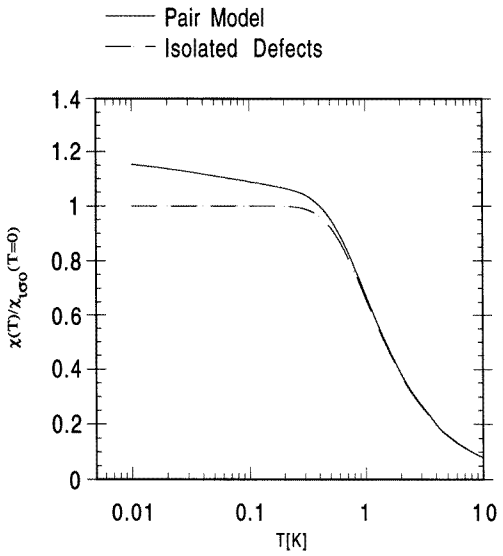

Figure 3. The dynamical susceptibility for an impurity pair, as obtained from equation (79). The dashed line gives the susceptibility of isolated defects.

8.2. Dielectric susceptibility

The dielectric response function is obtained from equations (36)–(38) by performing the averaging over all pairs and over the dipolar orientation:

$$\chi(\omega) = \frac{1}{3V}\sum_{\rm pairs}\alpha(\omega). \tag{78}$$

When assuming both signs of J to occur with equal probability, the terms proportional to sign(J) in equation (38) cancel. Noting that $w_+^2 = 1/(1+x^2)$, $w_-^2 = x/(1+x^2)$ and putting $p = qd/2$, we find for the zero-frequency susceptibility

$$\chi(\omega\to 0) = \chi_{\rm iso}\int_{x_1}^{x_2} {\rm d}x\ \frac{\mu}{(1-x^2)^2}\left\{\tanh\left(\frac{x\Delta_0}{2k_{\rm B}T}\right)\frac{1}{x} + \tanh\left(\frac{\Delta_0}{2xk_{\rm B}T}\right)x^3\right\} \tag{79}$$

where we have used the expression for non-interacting (or isolated) tunnelling impurities

$$\chi_{\rm iso}(\omega\to 0) = \frac{2}{3}\frac{np^2}{\epsilon_0\Delta_0}. \tag{80}$$

As for the specific heat, the expression in (79) cannot be integrated analytically; in figure 3 we show its temperature dependence, together with $\chi_{\rm iso}(\omega\to 0)$.

The zero-temperature susceptibility arising from the pair model exceeds that expected for isolated impurities, and it weakly increases with decreasing temperature even at low temperature, where $\chi_{\rm iso}$ is constant. According to figure 3 both features are confirmed by the data for KCl:CN (cf. [11]), thus proving the significance of the low-energy excitations η_-. (Note, however, that the uncertainty in density of about 10 per cent would permit us to adjust the zero-temperature susceptibility to the value of $\chi_{\rm iso}$.) Our result does not agree with that of reference [24].

Finally we consider the zero-temperature limit of the low-frequency susceptibility; putting $T = 0$ and assuming $\mu \ll 1$, the integral (79) yields [17]

$$\chi(\omega = 0) = \chi_{\rm iso}\left[1 + \mu(\log(J_2/\Delta_0) - 1/2)\right] \qquad \text{for } \mu \ll 1 \text{ and } T \to 0. \tag{81}$$

Hence the pair-model susceptibility exceeds that of isolated impurities by a factor $[1 + \mu(\log(J_2/\Delta_0) - 1)]$; this effect may be traced back to the growing spectral weight of low-energy excitations η_-.

Note, however, that at higher concentration, i.e. for μ approaching unity, the pair model breaks down, and interaction with more than one neighbour leads to strongly *decreasing* low-frequency susceptibility [14, 17, 20–23].

8.3. The Rabi frequency

Recently rotary echoes of lithium impurities in KCl have been investigated in great detail [10, 30]. The Rabi frequency of two nearby defect ions with effective tunnel energy $\eta_- = \Delta_0\Delta_0'/J$ and asymmetry Δ in an external field $\boldsymbol{F}_0\cos(Et/\hbar)$ is given by

$$\Omega = \frac{1}{\hbar}\frac{\eta_-}{E}\boldsymbol{P}\cdot\boldsymbol{F}_0 \tag{82}$$

where $E = \sqrt{\eta_-^2 + 4\Delta^2}$. The availability of two stable isotopes ^{6}Li and ^{7}Li permits a thorough investigation of the mass dependence of Ω. Studying all combinations of defect pairs, Weis *et al* have confirmed the isotope effect arising from $\eta_- = \Delta_0\Delta_0'/J$, with Δ_0 and Δ_0' being given by either $^7\Delta_0 = 1.1$ K or $^6\Delta_0 = 1.7$ K [10, 30].

Our result, equation (59), ensures that a strongly coupled pair of impurities with finite asymmetry Δ is well described by an effective two-state system with tunnelling energy η_- and asymmetry 2Δ, thus permitting us to use the well known theory of rotary echoes of two-level systems. Treating the actual problem of two interacting eight-state systems yielded results essentially identical to our equation (59) [30, 17].

8.4. Relaxation

As a most significant consequence, a finite asymmetry energy gives rise to a relaxational feature in the correlation spectrum (61) with amplitude $4\Delta^2/E^2$; the rate γ_l arises from coupling to acoustic lattice vibrations.

When investigating the relaxation spectrum of interacting lithium defects, Enss and Weis [29] found a surprising isotope effect for the relaxation rate. Taking into account the coupling of all N defects on the lattice, a relaxation feature of spin-diffusion type was shown to emerge, with a rate proportional to Δ_0^{-4}. Considering equation (63) and $\eta_- = \Delta_0^2/J$, we find the rate derived in the present paper to vary with Δ_0^4. Thus spin–spin relaxation and spin–lattice relaxation show an opposite isotope effect; this clear signature should permit us to determine the dominant relaxation mechanism of coupled substitutional defects.

9. Summary

In this paper we have extended our previous work on the pair model for substitutional defects [15] by taking into account both a finite asymmetry energy and phonon coupling. Here we summarize the main results.

(i) At sufficiently low density corresponding to $\mu \leqslant \frac{1}{10}$, the pair model provides a satisfying description of the interaction effects on specific heat and dynamical susceptibility, as shown in figures 2 and 3.

(ii) The low-energy states of a pair of coupled impurities reduce to an effective two-level system, as is obvious from equation (59), with an effective tunnel energy η_- and a bias given by twice that of a single impurity. These results are confirmed by the perturbative treatment of two coupled eight-state systems [30, 17]. The calculated density of states accounts well for specific heat data.

(iii) For $\mu \ll 1$ the interaction results in an excess susceptibility as compared to that for isolated impurities; low-frequency data on KCl:CN would seem to confirm this effect.

(iv) According to the known results for a two-state system, we find a relaxation feature whose rate varies with the fourth power of the tunnelling energy Δ_0.

Appendix A. Unitary transformation

In the basis (23), the transformation diagonalizing the symmetric defect pair is given by

$$U = \begin{pmatrix} U_{11} & U_{11} & 0 & 0 \\ U_{11} & -U_{11} & 0 & 0 \\ 0 & 0 & U_{33} & U_{34} \\ 0 & 0 & U_{43} & U_{44} \end{pmatrix} \tag{A1}$$

with entries

$$U_{11} = \frac{1}{2\sqrt{2}} \begin{pmatrix} -w_- & \mathrm{i}w_- & w_+ & \mathrm{i}w_+ \\ -\mathrm{i}w_+ & w_+ & \mathrm{i}w_- & w_- \\ w_+ & -\mathrm{i}w_+ & w_- & \mathrm{i}w_- \\ \mathrm{i}w_- & -w_- & \mathrm{i}w_+ & w_+ \end{pmatrix} \tag{A2}$$

$$U_{33} = \begin{pmatrix} 1/2 & 1/2 & 1/2 & 1/2 \\ 1/2 & 1/2 & -1/2 & -1/2 \\ -\mathrm{i}a_1 & \mathrm{i}a_1 & -\mathrm{i}/2 & \mathrm{i}/2 \\ \mathrm{i}a_1 & -\mathrm{i}a_1 & \mathrm{i}/2 & -\mathrm{i}/2 \end{pmatrix} \tag{A3}$$

$$U_{34} = \begin{pmatrix} 0 & 0 & 0 & 0 \\ 0 & 0 & 0 & 0 \\ -a_2 & a_2 & 0 & 0 \\ -a_2 & a_2 & 0 & 0 \end{pmatrix} \tag{A4}$$

$$U_{43} = \begin{pmatrix} \mathrm{i}a_2 & -\mathrm{i}a_2 & 0 & 0 \\ -\mathrm{i}a_2 & \mathrm{i}a_2 & 0 & 0 \\ 0 & 0 & 0 & 0 \\ 0 & 0 & 0 & 0 \end{pmatrix} \tag{A5}$$

$$U_{44} = \begin{pmatrix} a_1 & -a_1 & 1/2 & -1/2 \\ a_1 & -a_1 & 1/2 & -1/2 \\ 1/2 & 1/2 & -1/2 & -1/2 \\ 1/2 & 1/2 & 1/2 & 1/2 \end{pmatrix} \tag{A6}$$

where we have used the shorthand notation

$$a_1 = \frac{1}{2}(w_-^2 - w_+^2) \qquad a_2 = w_- w_+. \tag{A7}$$

References

[1] Narayanamurti V and Pohl R O 1970 *Rev. Mod. Phys.* **42** 201
[2] Bridges F 1975 *Crit. Rev. Solid State Sci.* **5** 1
[3] Gomez M, Bowen S P and Krumhansl J A 1967 *Phys. Rev.* **153** 1009
[4] Baur M E and Salzman W R 1969 *Phys. Rev.* **178** 1440
[5] Klein M W 1984 *Phys. Rev.* B **29** 5825 (erratum **31** 2528)
[6] Byer N E and Sack H S 1968 *J. Phys. Chem. Solids* **29** 677
[7] Klein M W 1966 *Phys. Rev.* **141** 489
[8] Lawless W N 1966 *Phys. Kondens. Mater.* **5** 100
[9] Dobbs J N and Anderson A C 1986 *Phys. Rev.* B **33** 4172
[10] Weis R, Enss C, Leinböck B, Weiss G and Hunklinger S 1995 *Phys. Rev. Lett.* **75** 2220
[11] Weis R 1995 *PhD Thesis* Ruprecht-Karls University, Heidelberg
[12] Kranjc T 1992 *J. Phys. A: Math. Gen.* **25** 3065
[13] Würger A 1994 *Z. Phys.* B **94** 173; 1995 *Z. Phys.* B **98** 561
[14] Enss C, Gaukler M, Tornow M, Weis R and Würger A 1996 *Phys. Rev.* B submitted
[15] Terzidis O and Würger A 1994 *Z. Phys.* B **94** 341
[16] Terzidis O 1995 *PhD Thesis* Ruprecht-Karls University, Heidelberg
[17] Würger A 1996 *From Coherent Tunnelling to Relaxational Dynamics (Springer Tracts in Modern Physics)* (Berlin: Springer) at press
[18] Grabert H and Schober H R 1996 *Hydrogen in Metals III* ed H Wipf (Berlin: Springer) at press
[19] Wang X and Bridges F 1986 *Phys. Rev. Lett.* **57** 1355
[20] Fiory A T 1971 *Phys. Rev.* B **4** 614
[21] Knop K and Känzig W 1972 *Phys. Kondens. Mater.* **15** 205; 1974 *Helv. Phys. Acta* **46** 889
[22] Potter R C and Anderson A C 1981 *Phys. Rev.* B **24** 677
[23] Enss C, Schwoerer H, Arndt D, von Schickfus M and Weiss G 1994 *Europhys. Lett.* **26** 289
[24] Klein M W 1989 *Phys. Rev.* B **40** 1918
[25] Mori H 1965 *Prog. Theor. Phys.* **33** 127
[26] Zwanzig R 1960 *J. Chem. Phys.* **33** 1338
[27] Dobbs J N 1985 *PhD Thesis* University of Illinois
[28] Rau S, Enss C, Hunklinger S, Neu P and Würger A 1995 *Phys. Rev.* B **52** 7179–95
[29] Enss C and Weis R 1996 private communication
[30] Weis R, Enss C, Würger A and Lüty F 1996 *Phys. Rev.* B at press